Proceedings of the 2004 IEEE
International Conference on Robotics & Automation
New Orleans, LA • April 2004

A Robotic System for Transrectal Needle Insertion into the Prostate with Integrated Ultrasound

Chad M. Schneider and Allison M. Okamura
Department of Mechanical Engineering
Johns Hopkins University
Baltimore, MD 21218
{cschneider, aokamura}@jhu.edu

Gabor Fichtinger
Center for Computer-Integrated Surgical Systems and Technology
Johns Hopkins University
Baltimore, MD 21218
gabor@cs.jhu.edu

***Abstract*— We have designed a minimally invasive medical device with the capability to insert a needle (or catheter) under transrectal ultrasound (TRUS) image guidance through the rectum and into the surrounding tissue, primarily the prostate. A partial sheath surrounds an ultrasound probe 210° around the circumference in order to remain attached to the probe but minimize interference with the ultrasound image. A needle is inserted through one of two parametric guides on the sheath; which guide depends upon the desired location of the needle and the presence of anatomy to be avoided. Our hypothesis is that by reducing the amount of tissue, muscle, and nerves in the path of the needle, this method, when compared to the perineal approach, will improve both the accuracy of the needle placement and the comfort to the patient. Experiments with a custom phantom prostate demonstrate that this device provides target accuracy comparable to the current perineal approach.**

Keywords-needle insertion; prostate; therapy; medical robotics; ultrasound probe; transrectal; urology;

I. INTRODUCTION

Prostate cancer is the second leading cause of cancer death among American men, claiming 30,000 lives per year in the United States [1]. Close to one million prostate biopsies are performed in the U.S. annually, and the estimated number of new prostate cancers detected in 2002 was 189,000 [3]. In addition to cancer, about 50% of men over 50 years old in the United States experience symptoms from Benign Prostate Hyperplasia [4], the enlargement of the prostate that can result in acute urinary retention and require surgery if left untreated [5].

In contemporary practice, prostate biopsy and most local therapies are executed via needles inserted into the prostate through the perineum or through the rectal wall (Fig. 1). Both access routes have been documented to be safe and well tolerated. There are several factors in deciding the optimal access route for any given prostatic needle intervention: the number of insertions, needle placement error, need for anesthesia, and risk of infection. Generally, for interventions involving only a limited number of needle insertions, like biopsy, transrectal access is preferable. Transrectal ultrasound (TRUS) has been the dominant imaging modality in the guidance of prostate biopsy and therapeutic interventions. In current practice, however, the probe is manipulated freehand inside the rectum, thereby causing variable deformation to the prostate and rendering transrectal needle placement imprecise and unpredictable. In answer to this clinical challenge, the main goal of our research is to provide accurate and predictable transrectal needle placement into the prostate under conventional TRUS guidance, in a safe and simple manner.

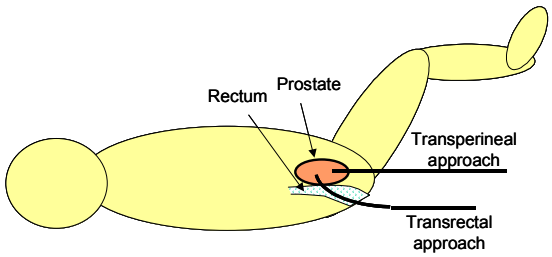

Figure 1. Two methods for introducing needles to the prostate: the transperineal approach and the transrectal approach.

The ultimate goal is to build a device that allows patients to undergo screening and therapy in the convenience of their doctor's office. Again, transrectal ultrasound imaging is desirable for this task because of its low cost, clinical popularity, simplicity, and real-time nature. Medical professionals are already familiar with this imaging modality

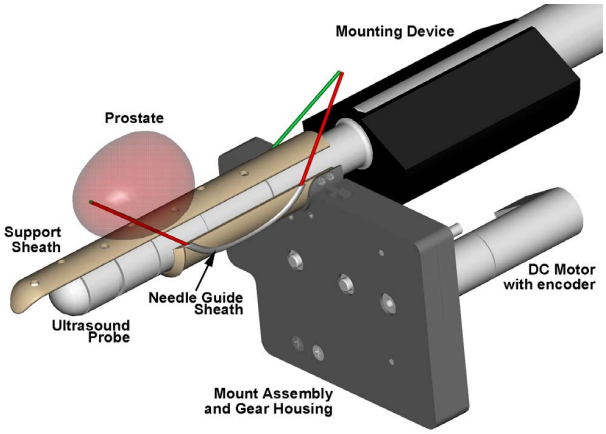

Figure 2. CAD assembly drawing of a parametric needle guide mounted on TRUS probe inserting a needle into the prostate. (Multiple needle guides provide a larger workspace.)

This work is sponsored by the National Science Foundation (grants EEC-9731478 and EIA-0312551) and Acoustic MedSystems, Inc.

and comfortable with the interface.

In addition to medical devices that minimize tissue deformation during needle insertion, there is recent work on needle insertion modeling that may also lead to more accurate targeting [6-8]. However, patient-specific tissue models will be required to make such planners feasible. Ideally, we would combine a medical device that minimizes tissue deformation with a tissue/needle model that predicts the remaining deformation in order to provide the most accurate needle placement. Since methods for acquiring patient-specific tissues models (e.g., elastography [9]) are not yet available or validated, our work in this paper concentrates on the design of a robotic device for inserting needles via paths that minimize deformation.

Our approach, therefore, is to integrate ultrasound imaging with a transrectally-introduced, 3-degree-of-freedom, (DOF), partially motorized robotic probe, shown in Fig. 2, providing accurate needle placement and greatly reducing contact with the muscles and nerves. The device is mounted to the ultrasound device, resulting in accurate registration of the needle end-effector with respect to the ultrasound image.

II. Device Design

A. Kinematics of the Device

We have employed a 3-DOF kinematic design related to previous systems developed at Johns Hopkins University [2, 10]. If the entry point on the cavity wall is not specified, then three decoupled degrees of freedom are necessary and sufficient for hitting an arbitrary target point given in Cartesian space, assuming the needle enters the tissue at some oblique angle across the cavity wall. These degrees of freedom are: translation of the needle guide sheath in the cavity, D_d, rotation of the needle guide sheath inside the cavity, ψ, and insertion depth of the needle, N_d. To determine these values, we calculated the inverse kinematics of the device geometrically, as shown in Fig. 3. We begin with a relationship between the needle exit angle and needle tip position:

$$\tan(\xi + \psi + d) = \frac{P_z}{P_x}. \quad (1)$$

Solving for ψ gives the rotation of the needle guide sheath inside the cavity:

$$\psi = \arctan 2(P_z, P_x) - \xi - d. \quad (2)$$

Now we solve for the depth of needle and device insertion. The Law of Cosines gives

$$c^2 = a^2 + \lambda^2 - 2a\lambda\cos(b) \quad (3)$$

and the Pythagorean Theorem gives

$$c^2 = P_x^2 + P_z^2. \quad (4)$$

Combining (3) and (4) yields

$$P_x^2 + P_z^2 = a^2 + \lambda^2 - 2a\lambda\cos(b), \quad (5)$$

and rearranging (5) leads to the polynomial

$$0 = \lambda^2 + 2a\lambda\cos(b) + (a^2 - P_x^2 - P_z^2). \quad (6)$$

This polynomial has one positive and one negative root. The positive real root is the 2-dimensional projection of the insertion depth for the needle,

$$N_d = \frac{\lambda}{\sin(\lambda)}, \quad (7)$$

where ζ is the angle between the needle and the y-axis (into the page) in Fig. 3. The insertion depth of the needle is coupled with the insertion depth of the device to achieve the desired P_y position:

$$D_d = P_y - N_d\cos(\zeta). \quad (8)$$

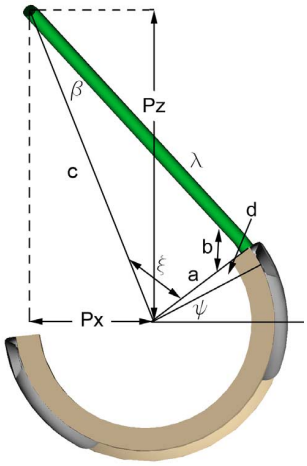

Figure 3. Geometric diagram of the device for calculation of the inverse kinematics.

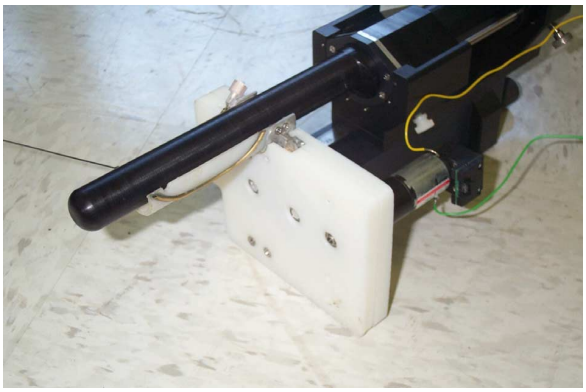

Figure 4. Prototype of geared assembly, integrated with an Interplant® stepper.

B. Compatibility With Ultrasound Imaging

The device is a 3-DOF partially encoded needle guide that is spatially coupled with an existing transrectal ultrasound stepper. In the current embodiment, this is the interplant® stepper (Burdette Medical Systems), for which the mounting configuration replicates the mounting of a standard brachytherapy template and is easily exchangeable. The needle insertion device is fully compatible with the transrectal ultrasound system employed in the interplant® system, in order to increase the applicability of our needle insertion device. The needle guide was not built inside or attached to the ultrasound probe because it is not feasible to modify a commercially available ultrasound probe. Therefore, we designed a suitable guiding conduit for the needle outside the US probe.

C. A Novel Needle Path

The solution we have developed is a parametric-curve needle-guide along the ultrasound (US) probe, Fig. 4, made of Nylon 66 because of its biological compatibility. The challenge was to lead the needle along a path within a conduit, the curvature of which is kept under limits dictated by the elastic properties of the needle to be inserted. A nitinol needle, an alloy comprised of nickel and titanium, was used for this application specifically because of its exceptional elastic properties. The curvature of the needle through the needle guide stays within the elastic range of the needle. This allows a straight and predictable exit trajectory, at a repeatable 38° angle to the axis of the sheath.

D. The Operational Workspace

Since the curve is not in the plane containing both the target and the axis of rotation of the probe, it is difficult to achieve a comprehensive workspace with just one guide that is capable of avoiding sensitive anatomy. Therefore, two winding guides divide the workspace (Fig. 5), avoiding the nerve bundles that run parallel to the rectum. The control algorithm assigns points left of the center of rotation to the right needle and vice versa.

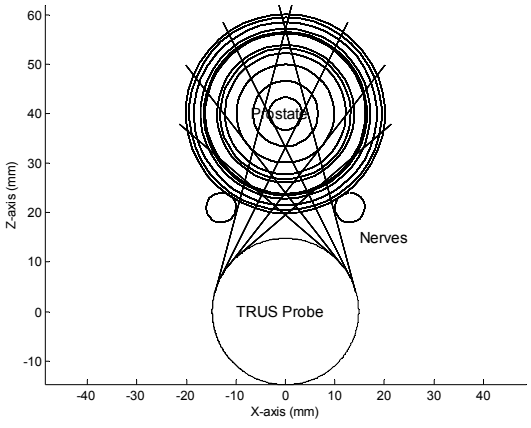

Figure 5. Axial view of the reachable workspace inside the prostate.

It is noteworthy that this approach significantly differs from the needle guides presented in [2] and [10], where the designers were not constrained by any mechanical components a priori present inside the rectum.

E. The Current Prototype

In our prototype, shown in Fig. 4, brass guides are rigidly mounted on a half cylinder sliding and rotating on the TRUS probe. Because we use a partial sheath around only 210° of the probe, the outer diameter of the sheath is as small as 24.2mm and as large as 28.0mm. While the needle guides add approximately 1.2mm to the largest radius, this additional size only affects patient comfort during insertion, where the guides are 180° across from each other. After insertion, the paths of the guides approach each other, decreasing their effect on the maximum diameter. The TRUS probe has an outer diameter of 22.3mm. The parametric curves were milled into the half-sheath using a ball-end mill on a 4-axis CNC mill. The brass guides were bent to form and glued onto the half-sheath using Master Bond EP21ND 2-component epoxy, because of its food grade and USP Class VI certification. The half cylinder is open on the anterior side of the rectum, to avoid degradation of ultrasound signal from the prostate. We use a geared drive with an encoded dc motor (Maxon Precision Motors, Burlingame, CA) to reference the half-sheath with respect to the ultrasound base. Currently, both the insertion depth of the device and that of the needle is measured by hand, but adding a motor/encoder to the interplant® stepper would negate the advantage of integrating seamlessly with current devices.

The motor driving the half-sheath is a dc, 6 Watt, A-max 22, graphite brush type with a maximum torque of 7.19 mN-m. It is combined with a planetary gearhead GP 22 A, 19:1, and a 2-channel, 100 counts-per-turn, digital encoder. This motor was chosen because of its torque specification and the ratio of the planetary gearhead. We estimated the force of friction on the half-sheath and combined that with the ratios of all the rotational linkages to determine a rough specification for the motor.

Brass gears (Stock Drive Products, New Hyde Park, NY) mounted to stainless rods rotate on ABEC-5 sealed ball bearings inside the two-piece gear housing. The gears provide a 4:1 mechanical advantage to the motor, allowing the motor to drive closer to its preferred operating range. One of the brass gears was milled to fit the outer-radius of the half-sheath aluminum drive.

The gear housing, half-sheath, and motor attach to the interplant® stepper by the ball-screw and locating pin used in the standard perineal template shown in Fig. 5. The standard template just screws off the end and our device screws onto the end of that ball-screw.

Once the prototype was built, we noticed that when the guiding curves in Fig. 3 move into a cavity such as the rectum, the guide holes could accidentally cut the rectum surface and holes could also trap infectious rectal debris that

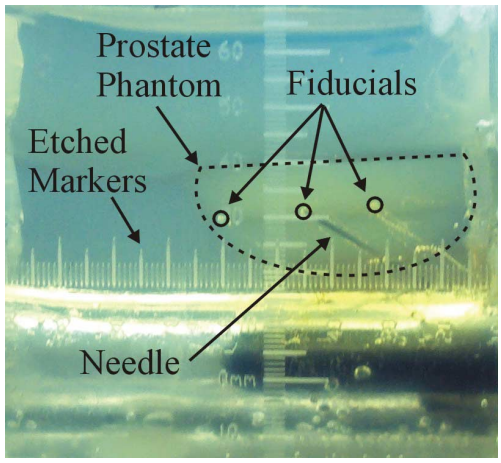

Figure 6. The phantom prostate. The "prostate" is outlined with a dashed line and the teflon fiducials are highlighted with circles. Laser-etched markers allow measurement of the three-dimensional Cartesian locations of the target and needle end-point.

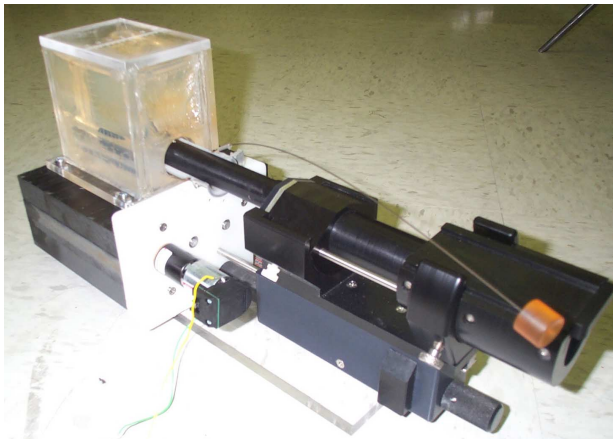

Figure 7. Experiment setup with a phantom prostate. Laser-etched measures provide three dimensional Cartesian location of the target and needle end-point.

might get transferred into tissue by the needle. As a protective measure, a rounded hump will lead the needle guides into the rectum in future prototypes.

III. Experimental Evaluation

A. Experimental Setup

To quantify the performance of the device in comparison with standard methods of needle insertion into the prostate, we developed a phantom prostate. This phantom prostate, shown in Fig. 6, was created using clear Super-Soft Plastic with Plastic Softener (M-F Manufacturing, Fort Worth, TX), combined in ratios of 4:1 for the prostate and 1:1 for the surrounding tissue. Three 1.58mm Teflon balls were inserted into the prostate during the molding process to serve as targets during the experiment. Laser-etched markings on the sides of the phantom provide Cartesian locations in 1mm increments. A particular measurement was achieved by

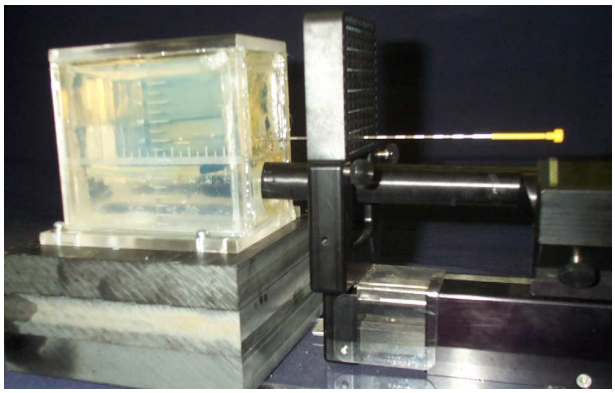

Figure 8. Experiment setup with the phantom prostate using the template approach of inserting a straight needle through the perineum.

making a sight-line of three points: a measurement etch, its identical counterpart on the opposite side, and the target. Lining up these three points ensures that the target is in the plane of the measurement etches. Teflon was used as the targets because of its visibility under CT, in case visual measurement proved too difficult and for use in future experiments.

B. Experimental Task

1) Transrectal Experiment

To begin the experiment, the Cartesian coordinates of the targets were identified using the measurement etchings on the phantom prostate as described in section III-A. These values were input to the control program as the desired end-effector location, and the required joint positions to reach the target were determined from the inverse kinematics of the device. The three joint positions describe the translation and rotation of the needle guide and the insertion depth of the needle. The device was inserted into the phantom prostate (Fig. 7), and the control program read the motor encoder to determine the rotation of the needle guide. The angle of the sheath was computer-controlled to achieve the desired angle. A constant velocity trajectory and proportional-derivative (PD) controller was used to control the motion of the sheath. The insertion depth was set using the translation stage on the interplant® stepper. Finally, a 1.2 mm (18 gauge) diamond-tip nitinol needle was inserted to the proper depth. The operator did not look at the location of the target during this procedure, lest visual feedback inadvertently cause small changes in the insertion. Six insertions were made for the three points, one from each of the two guides. Only these six insertions were collected to avoid any adverse effects from previous needle paths.

2) Transperineal Experiment

For the traditional transperineal, or template, approach shown in Fig. 8, our robotic device was exchanged on the interplant® stepper for the standard perineal template. The template was lined up in front of the phantom prostate. The kinematics of the template are decoupled into Cartesian coordinates, so no transformation was necessary. A 1.2mm (18 gauge) diamond-tip stainless steel straight needle, marked in 5mm increments, was then inserted to the target

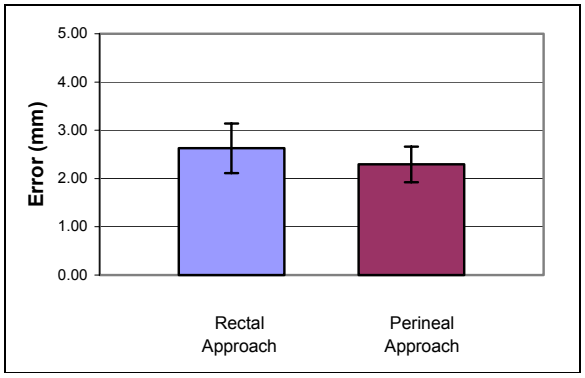

Figure 9. Comparison of the needle placement accuracy of the two approaches (p = 0.30).

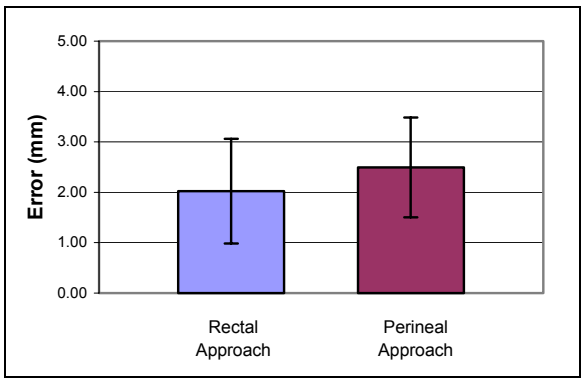

Figure 10. Comparison of the tissue deformation and resulting target location (p = 0.51).

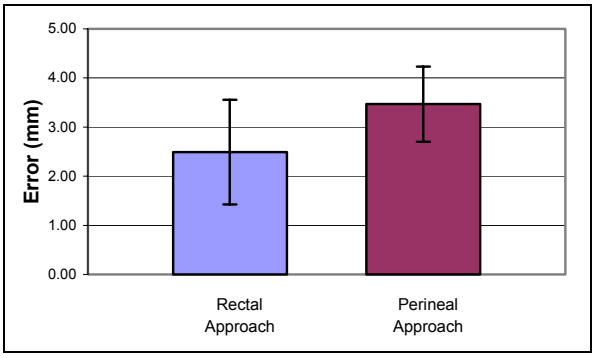

Figure 11. Comparison of the distance between the target and the needle endpoint (p = 0.16).

depth. Five insertions were made. Since the template has a grid of holes spaced 5mm apart in two directions, targets could easily fall between the discrete locations of the holes. Thus, the two closest points were chosen for two of the targets. The third target lined up well with one hole in the template, so only that point was chosen. These data points were carefully collected and statistically analyzed for significant differences.

IV. Results and Discussion

A. Analysis of the Data

After compiling the data, we used several methods to characterize the differences between the two approaches. First, needle placement accuracy, shown in Fig. 9, is approximately equivalent for each approach, with p = 0.30 from a single-factor ANOVA test. This represents how well the needle can be placed at a specified location in space. This result is encouraging, because it indicates that our initial prototype provides needle placement as accurate as the state of the art in medical practice.

As seen in Fig. 10, the amount of tissue deformation from the rectal approach is shown to be slightly less than that of the perineal template approach. However, ANOVA proved the difference to be statistically insignificant with p = 0.51. The end result, shown in Fig. 11, is that accuracy is a product of both needle placement and tissue deformation. The convention for statistical significance is usually p = 0.05, correlating to 95% confidence that the data is different. For the data shown in Fig. 11, p = 0.16, so we cannot be as confident in this difference as we hoped. However, this p-value does give us 84% confidence. Improvement of the experimental procedure might increase the accuracy of our results and the difference in data between the two approaches.

B. Future Work

One of the most significant problems in TRUS-guided prostate interventions is variable deformation of the prostate caused by the transducer translating in and out the rectum. To eliminate this problem, we would like to decouple the rectum and the transducer mechanically, by inserting a cantilevered support sheath (Fig. 12) into the rectum above the TRUS probe. The sheath extends slightly beyond the prostate base, to provide imaging access and mechanical support to the entire gland and relevant anatomy. The TRUS probe will move freely below the sheath, greatly reducing any normal force onto the prostate through the rectum wall. The sheath will be rigidly affixed to the ultrasound stepper base, although this mounting configuration has yet to be designed. Alternatively, it could be loosely placed into the rectum and still provide support to the prostate. In either case, the rectum will not be subjected to variable normal force or friction, so the prostate will not deform during imaging. The sheath will somewhat reduce the ultrasound signal coupling between the TRUS probe and the rectum wall, although this has been mitigated by our design. The sheath has a plurality of holes in it to minimize interference

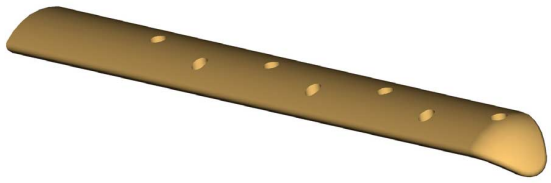

Figure 12. CAD view of the protective rectal support sheath.

with the ultrasound signal by facilitating the flow of coupling gel during movement of the probe.

A few small improvements must be made to the prototype before further testing can take place. A rounded hump must be added to front edge of the half-sheath to protect the patient from the sharp edges of the needle guides. Friction in the gearbox must be reduced with better control of the tolerances to allow for accurate computer control of the angle. A prostate support should be integrated into the device. The phantom prostate should also be improved to include more realistic tissue, inhomogeneity, and muscles. With these improvements, we hope that future testing will prove this device can provide a needle pathway that penetrates less muscles, nerves, and tissue than the standard perineal approach, thereby reducing the amount of pain, tissue deformation, and target displacement currently seen in prostate needle insertion.

V. Conclusion

We have developed a device to integrate a new method for needle insertion with an ultrasound probe. Our experimental data demonstrates that this device is at least as accurate as the standard approach with a straight needle through the perineum and a brachytherapy template. Other possible benefits of the device, such as reduced pain and healing time, are also advantages of our approach.

In the long term, an ideal needle insertion approach would combine mechanical device design and control with patient-specific tissue deformation modeling. Methods typically used to model tissue deformation, such as finite element analysis (FEA), are best used for small deformations. Thus, a device that decreases the amount of tissue deformation during needle insertion will make it feasible to use these tissue models to predict the remaining (minimal) deformation. Work on needle steering after the needle enters the tissue, such as externally applied forces to purposely deform the tissue or the use of bevel tip asymmetry to bend the needle path, will also improve the accuracy of needle targeting.

VI. Acknowledgments

The authors would like to Dr. Burdette for the loan of several pieces of equipment for extended time periods, which allowed us to build a working prototype.

VII. References

[1] American Cancer Society. “What are the key statistics about prostate cancer?” http://www.cancer.org/docroot/CRI/content/CRI_2_4_1X_What_are_the_key_statistics_for_prostate_cancer_36.asp; accessed Dec 9, 2003.

[2] G. Fichtinger, A. Krieger, R. C. Susil, A. Tanacs, L. L. Whitcomb, and E. Atalar, “Transrectal prostate biopsy inside closed MRI scanner with remote actuation, under realtime image guidance,” Fifth International Conference on Medical Image Computing and Computer-Assisted Intervention, Lecture Notes in Computer Science 2488, Part 1, Springer, 2002, pp 91-98.

[3] A. Jemal, A. Thomas, T. Murray, and M. Thun, “Cancer statistics,” CA: a Cancer Journal for Physicians, 2002, Vol. 52, No. 1, pp. 23-47.

[4] R. S. Kirby and J. D. McConnell. “Benign Prostatic Hyperplasia”, 2nd ed. Oxford: Health Press Limited, 1997, pp. 10-12.

[5] J. D. McConnell, “Epidemiology, etiology, pathophysiology, and diagnosis of benign prostatic hyperplasia,” *Campbell's Urology*, 7th ed., Vol. 2., P. C. Walsh, *et al.*, eds., Philadelphia: WB Saunders Company; 1998, pp. 1429-1452.

[6] R. Alterovitz, J. Pouliot, R. Taschereau, I.-C. J. Hsu, and K. Goldberg, “Sensorless planning for medical needle insertion procedures,” IEEE/RSJ International Conference on Intelligent Robots and Systems, 2003, pp. 3337-3343.

[7] S. P. DiMaio and S. E. Salcudean, “Needle insertion modeling and simulation,” IEEE Transactions on Robotics and Automation, Vol. 19, No. 5, 2003, pp. 864 –875.

[8] A. M. Okamura, C. Simone and M. D. O'Leary, “Force modeling for needle insertion into soft tissue,” IEEE Transactions on Biomedical Engineering, 2004. (in press)

[9] D. B Plewes, J. Bishop, A. Samani, and J. Sciarretta, “Visualization and quantification of breast cancer biomechanical properties with magnetic resonance elastography,” Physics in Medicine and Biology, Vol. 45, No. 6, 2000, pp. 1591-1610.

[10] R. C. Susil, A. Krieger, J. A. Derbyshire, A. Tanacs, L. L. Whitcomb, E. R. McVeigh, G. Fichtinger, and E. Atalar, “System for MR image–guided prostate interventions: canine study,” Radiology, Vol. 228, No. 3, 2003, pp. 886-894.